SINGLE-CRYSTAL SUPERALLOY JOINING

Akane Suzuki, Jeffrey Schoonover, Chen Shen, David Wark

GE Global Research; 1 Research Cr., Niskayuna, NY 12309, USA

Abstract

A new process route of diffusion brazing has been identified for joining Ni-base single-crystal superalloys. This process was developed through an understanding of microstructure evolution observed during conventional diffusion brazing of a single-crystal superalloy René N5 with interlayer materials containing B as a melting point depressant. It was found that the interlayer does not fully melt during high temperature joining heat treatment due to the fast diffusion of B from the interlayer into the substrate, and that grain coarsening, instead of epitaxial growth, is responsible for producing joints free of bond line. A new two-step joining heat treatment process route was established to effectively use grain coarsening and minimize the formation of the grain defects. Diffusion calculations were applied to predict the distribution of B and thus avoid incipient melting during the heat treatments. The René N5 joined by the new process demonstrated high temperature tensile properties equivalent to those of the single-crystal René N5, and the joined specimens did not fail at the joints.

Introduction

Diffusion brazing, also known as transient liquid phase bonding, has been recognized as a potential process to produce joints with excellent high temperature strength compared with other joining methods such as brazing and welding, and it has been explored for joining Ni-base superalloy components used in aircraft engines and power generation gas turbines [1-2]. Application of diffusion brazing to single-crystal superalloy components can provide opportunities to enable complex component architectures that cannot be made by traditional casting processes [3-6].

Compared with other joining methods, diffusion brazing has an advantage in producing mechanically more reliable joints for single-crystal superalloys. Other processes, for example, brazing and welding, result in a formation of polycrystalline microstructure, and the joints cannot provide high temperature mechanical strength compatible with the single-crystal parent materials. Diffusion bonding can retain the single-crystal structure across the bond line, however, it typically requires high load (up to 100 MPa) during the bonding process and very tight tolerance in conditioning the mating surfaces. Because diffusion brazing involves melting of the interlayer material, it typically requires only a small load up to 2 MPa [2], unlike diffusion bonding.

Diffusion brazing process typically uses an interlayer material containing elements that are melting point depressants as well as fast diffusers, and the process is typically described as follows: (1) the interlayer melts during heating to a temperature above its melting point, (2) the interlayer solidifies isothermally as the melting point depressants diffuse away into the substrate, (3) the substrate material epitaxially grows through the joint [1-6].

Successful diffusion brazing of single-crystal superalloys can maintain single-crystal structure across the joint, however the process often leaves microstructural defects, such as isolated grains along the joints, which are detrimental to the mechanical properties of the single-crystal materials.

B, Si and P are the most widely used elements as melting point depressants in the interlayer materials used for conventional brazing and diffusion brazing processes [1-6]. Other metallic elements, such as Mn and Ge [7-9], can be also used. In this study, B was chosen as a melting point depressant. Among the elements considered, the diffusion of B is the fastest, which is important for raising the melting temperature of the joint after joining is complete. An addition of 1 wt% B to a Ni-base superalloy lowers the solidus temperature by about 130 °C, which is more efficient than other melting point depressants. Furthermore, B is one of the typical constituents in Ni-base single-crystal superalloys.

There have been many studies on the kinetics of diffusion brazing of polycrystalline superalloys with relatively low-alloyed interlayer materials containing high amounts of B and/or Si [10-15]. They were mostly focused on the isothermal solidification and phase formation, and there is a lack of understanding of the evolution of grain structure and the change in the distribution of the melting point depressants, especially B. These are critical factors for joining single-crystal superalloys, because controlling grains to maintain the single-crystal structure across the joint and diffusing away the melting point depressants are the key requirements to produce joints with high temperature mechanical strength.

In this study, microstructure evolution during diffusion brazing of a Ni-base single-crystal superalloy was investigated using interlayer materials containing B to understand the changes in the grain structure and the distribution of B. Based on the observations, an improved joining heat treatment process was developed. Mechanical properties of the joined single-crystals were evaluated in comparison with a single-crystal material.

Experimental Procedures

A second generation Ni-base single-crystal superalloy René N5 (Ni-7.5Co-7Cr-1.5Mo-5W-3Re-6.2Al-6.5Ta-0.15Hf-0.05C-0.04B, wt%) was used for the joining experiments. Coupons were prepared from a single-crystal slab after the standard full solution heat treatment. The mating surfaces were perpendicular to the crystal growth orientation close to [001], and the mating surfaces were finished by low stress grinding. Foils containing 2~3 wt% B were used as the interlayer materials. The thickness of the foils was about 50 μm. For the microstructure study, the René N5 coupons and the interlayer foil were placed in a bolted fixture to keep them in place during the heat treatments. For preparing

mechanical property evaluation specimens, a pressure up to 2 MPa was applied during the joining process. After the joints were subjected to the standard solution and three-step aging treatments, tensile specimens were extracted. Round bar specimens with a gage length 19 mm and a gage diameter 4 mm were machined. The joint was placed in the middle of the gage section, normal to the [001] loading direction. Tensile tests were conducted at room temperature, 760, 982 and 1093 °C in air. Specimens of the single-crystal René N5 with [001] orientation were tested at the same conditions for comparison.

Results and Discussion

Microstructure Evolution during Joining Process

Figure 1 shows a typical example of the grain defects formed at the joints after a typical diffusion brazing heat treatment. The coupons of single-crystal René N5 and a conventional diffusion brazing interlayer foil containing 3 wt% B (Ni-8Co-9Cr-4W-2Al-4Ta-1Hf-3B, wt%) were heated at 10 °C/min to 1280 °C and held at the temperature for 4 hours. Chains of grains were frequently observed along the joint together with regions that showed no bond line. In single-crystal superalloys, presence of grain boundaries degrades mechanical properties.

To understand the mechanism of the grain defect formation during the diffusion brazing process, evolution of the grain structure and the distribution of B were studied by conducting a series of interrupted heat treatments. The same substrate and interlayer materials were used. The solidus and liquidus temperatures of the interlayer foil were 1067 and 1103 °C, respectively. Two coupons with the interlayer placed between were heated to selected temperatures between 1050 and 1250 °C at 10 °C/min, and held at the target temperatures for 5 min, followed by water quench.

Figure 2 shows backscattered electron images and the corresponding concentration maps of B generated by electron microprobe analysis (EPMA). In most cases, the two coupons were separated during water quench due to their immature state of metallurgical bonding, and the images shown were taken from the substrate coupon with the interlayer still attached. At 1100 and 1150 °C, the joint regions showed coexistence of spherical solid particles and liquid matrix phase (Figs. 2a~2d), despite the fact that the interlayer should be close to or fully molten based on its liquidus temperature. B mainly partitioned to the liquid matrix, and its concentration was low in the solid particles. Some solid particles were deposited on the substrate surfaces, and they started growing into the substrate (Fig. 2c). Grain boundaries were clearly observed in the substrate near the joint. Significant diffusion of B into the substrate up to about 30 μm deep was observed in the B concentration maps (Figs. 2b and 2d). With increasing temperature, the grains grew deeper into the substrate (Fig. 2g). B concentration in the substrate near the joint decreased due to its further diffusion into the substrate (Figs. 2f and 2h), but localized regions with high B concentration were observed along the grain boundaries (Fig. 2h).

Based on this series of heat treatments, the following key observations were made: (1) significant diffusion of B into the substrate occurs during heating, (2) the interlayer never fully

Figure 1. Microstructure of the René N5 coupons joined with the Ni-8Co-9Cr-4W-2Al-4Ta-1Hf-3B interlayer foil at 1280 °C/4 hours, showing the typical grain defects.
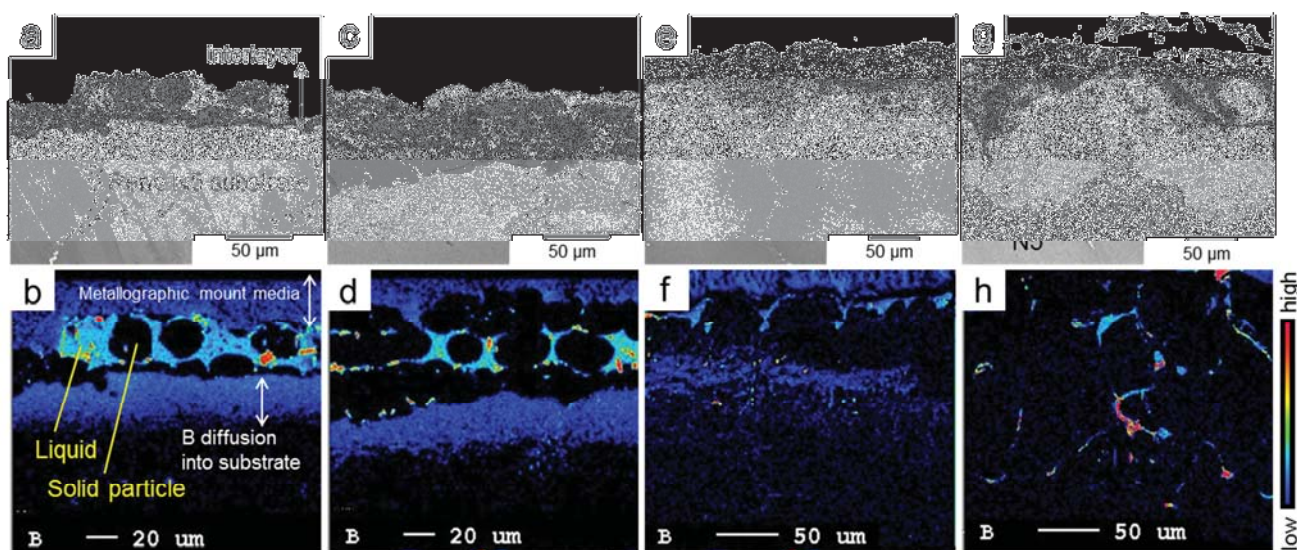

Figure 2. Backscattered electron images showing partial melting of the interlayer (a, c, e, g) and corresponding B concentration maps showing distribution of boron (b, d, f, h) during diffusion brazing. Specimens were heated at 10 °C/min to (a, b) 1100 °C, (c, d) 1150 °C, (e, f) 1200 °C and (g, h) 1250 °C, then held for 5 min followed by water quench.

334

melts, even at temperatures above the liquidus temperature of the interlayer, due to the early loss of B into the substrate, and (3) there is no epitaxial growth of grains, which had been counted on for restoring the single-crystal structure in the diffusion brazing process. The solid particles at the joint region never disappeared during the heating. Therefore, it is more likely that the disappearance of grains along the joints during diffusion brazing of a single-crystal superalloy is caused by elimination of the interlayer grains by grain coarsening, not by epitaxial growth of the substrate single-crystal material. However, when the interlayer grains become too large to be eliminated by grain coarsening (ex. Fig. 2b), they will remain as grain defects along the joints, resulting in a microstructure similar to the one shown in Fig. 1.

Improved Joining Heat Treatment

The above observation indicates that it is necessary to promote growth of the substrate single-crystal grains to efficiently eliminate the grains in the joint region to produce a single-crystal joint that is free of grain defects. In grain coarsening, small grains tend to be eliminated to lower the grain boundary surface energy in the system. Mobility of grain boundaries can be enhanced by reducing obstacles, such as precipitates. A two-step joining process was attempted to form small grains at the joint and then to minimize precipitates for grain coarsening. The first step was a low-temperature heat treatment at a temperature above the solidus temperature of the interlayer, followed by furnace cool. The purpose of this step is to partially melt the interlayer, but keep the size of the solid particles as small as possible. The second step was a high-temperature heat treatment at a temperature near or above the γ' solvus temperature of the substrate material. The mobility of grain boundaries is expected to be improved by the temperature and the minimum amount of the γ' particles present.

Figure 3 shows microstructures of René N5 coupons joined with the Ni-8Co-9Cr-4W-2Al-4Ta-1Hf-3B interlayer foil after the first and second steps. After the first step at 1150 °C for 1 hour with an applied pressure of 1 MPa (Fig. 3a), the joint region between the single-crystal substrates showed grains about 20 μm thick and up to 100 μm wide. After the second high-temperature heat treatment at 1270 °C for 24 hours without an applied pressure (Fig. 3b), the joint region exhibited no bond line or grain defects. The grains formed in the first step were wide along the lateral direction, but thin enough along the longitudinal direction (Fig. 3a).

The same two-step heat treatment process was applied to the coupons of René N5 with a different interlayer foil containing 2% B (Ni-7.5Co-7Cr-1.5Mo-5W-6.2Al-6.5Ta-0.15Hf-2B, wt%). The chemistry of the interlayer was selected based on the composition of René N5, and this material is hereafter referred as N5+2B. Its solidus and liquidus temperatures were 1106 and 1260 °C. At 1150 °C, the interlayer partially melted, and the joint region showed fine grains about 5 μm in size (Fig. 4a). After the second step, the grains at the joint were completely eliminated (Fig. 4b). The two-step heat treatment worked regardless of the interlayer chemistries used in this study.
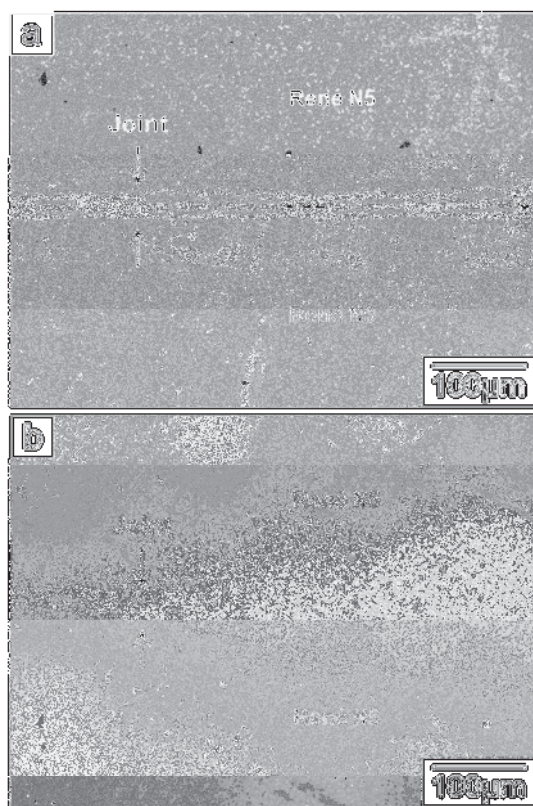

Figure 3. Microstructure of the René N5 coupons joined with the Ni-8Co-9Cr-4W-2Al-4Ta-1Hf-3B foil using the two-step joining heat treatment: (a) 1150 °C, 1 MPa for 1 h, FC and (b) 1270 °C for 24 h, FC.
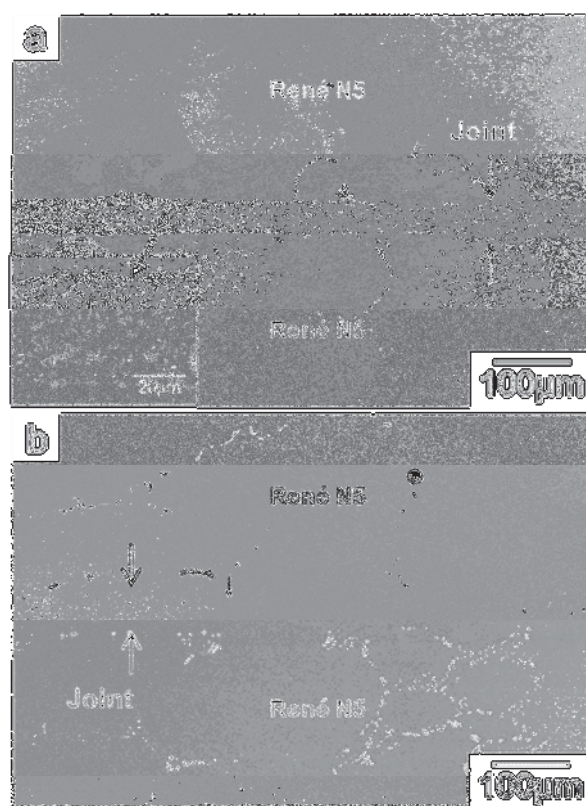

Figure 4. Microstructure of the René N5 coupons joined with the N5+2B interlayer foil using the two-step joining heat treatment: (a) 1150 °C, 1 MPa for 1 h, FC, and (b) 1270 °C for 24 h, FC.

Mitigation of Incipient Melting

Due to the diffusion of B from the interlayer into the substrate, the substrate near the joint becomes susceptible to incipient melting during the second step heat treatment. Figure 5 shows a microstructure of the René N5 coupons joined with the N5+2B interlayer foil. After the first step heat treatment at 1150 °C, the specimen was heated up to 1270 °C at 10 °C/min, followed by water quench without hold. Adjacent to the joint, there was a zone about 50 μm deep containing eutectic borides, which indicate the occurrence of incipient melting. In this zone, the interdendritic TaC carbide particles in the René N5 substrate were dissolved.

To determine the incipient melting temperature, the René N5 coupons joined with the N5+2B interlayer foil was heated at 10 °C/min to 1200, 1225 and 1250 °C, and held for 4 hours, followed by water quench. The interdendritic TaC particles were intact up to 1225 °C without dissolution (Figs. 6a and 6b). The incipient melting associated with the formation of the eutectic borides was observed at 1250 °C (Fig. 6c). Therefore, the incipient melting temperature is between 1225 and 1250 °C when specimen is heated at 10 °C/min. These observations indicate that incipient melting can be avoided by lowering the B concentration near the joint and increasing the incipient melting temperature higher than the second step heat treatment temperature, 1270 °C.

To understand the distribution of B during the joining process, diffusion calculations were performed using the half of the geometry (25 μm interlayer and 475 μm substrate) (Fig. 7a). Using TCNi5 and MobNi2 databases [16-17] with modified B mobilities (reduced about 10 times) based on a prior comparison study with semi-quantitative EPMA data, the elemental profiles were calculated following the joining heat treatment cycles. Diffusion below 900 °C was omitted from the calculations. Figure 7b shows the distribution of B after the first step heat treatment at 1150 °C, followed by heating at 1 °C/min to 1270 °C. The local melting temperatures were calculated based on the local

compositions in the calculated elemental profiles (Fig. 7c). The predicted B concentration profile (Fig. 7b) shows a fluctuation (0~1.7 wt%) at the interface between the interlayer and the substrate. The fluctuation was associated with a predicted boride phase in that region, which however was not observed in the actual specimen along the interfaces (Fig. 5), nor on the EPMA boron profile. It is likely an artifact of the thermodynamic prediction for boride phases, or due to slow kinetics of the boride formation during a relatively transient diffusion process. Excluding the fluctuation in the profile, the B concentration is the highest in the joint region (~0.5 wt%) and becomes comparable to the substrate at approximately 200 μm away from the joint region (Fig. 7b). The local melting temperature follows the B concentration profile. It is the lowest in the joint region (~1260 °C), and increases with the distance from the joint region. The lowest local melting temperature predicted in the joint region was considered as the incipient melting temperature in this condition.
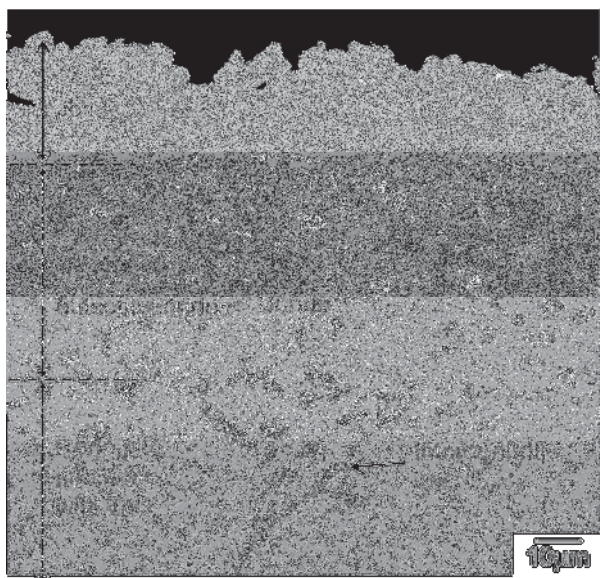

Figure 5. Microstructure of the René N5 coupons joined with the N5+2B interlayer foil. The specimen was heat treated at 1150 °C for 1 h, FC, followed by 10 °C/min to 1270 °C, WQ.
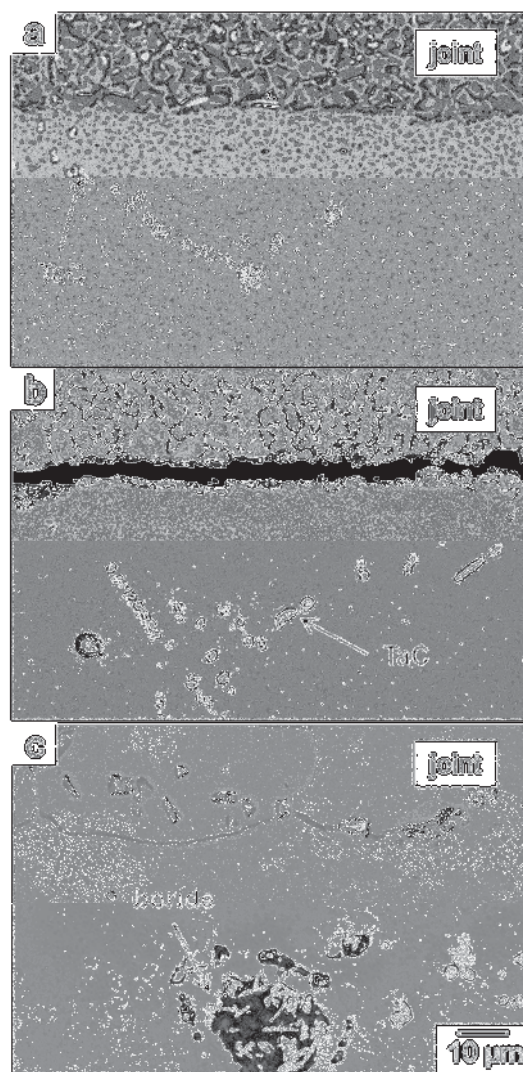

Figure 6. Microstructure of the René N5 coupons joined with the N5+2B interlayer foil. The specimens were heat treated at 1150 °C for 1 h, FC, followed by 10 °C/min to (a) 1200 °C/4 h, (b) 1225 °C/4 h and (c) 1250 °C/4 h.
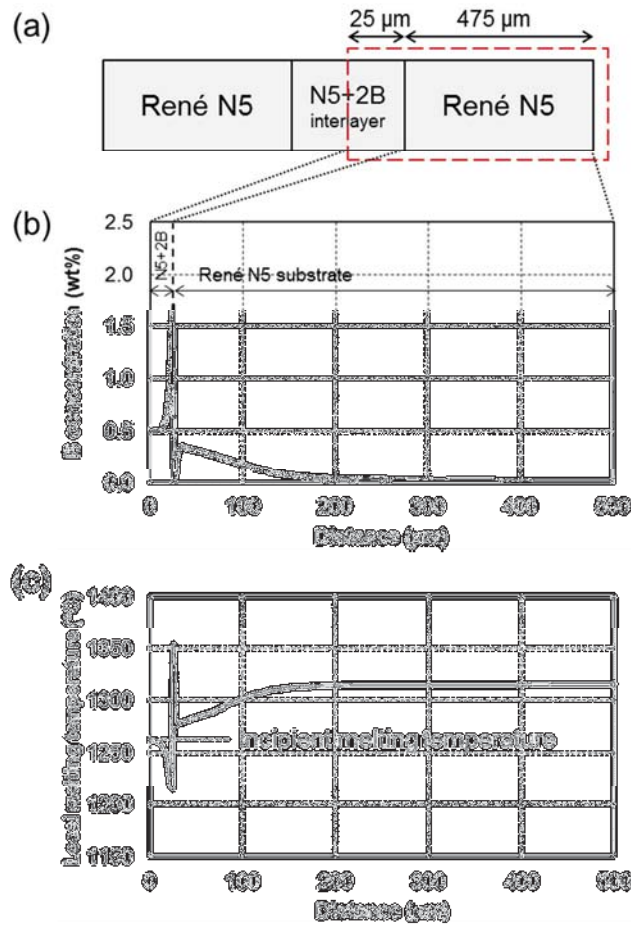
Figure 7. (a) A schematic of the joined René N5 with the N5-2B interlayer, (b) the predicted distribution of B and (c) the corresponding local melting temperature after the following heat treatment cycle: heating at 10 °C/min to 1150 °C, hold for 1 h, FC at 10 °C/min, followed by heating at 1 °C/min to 1270 °C.
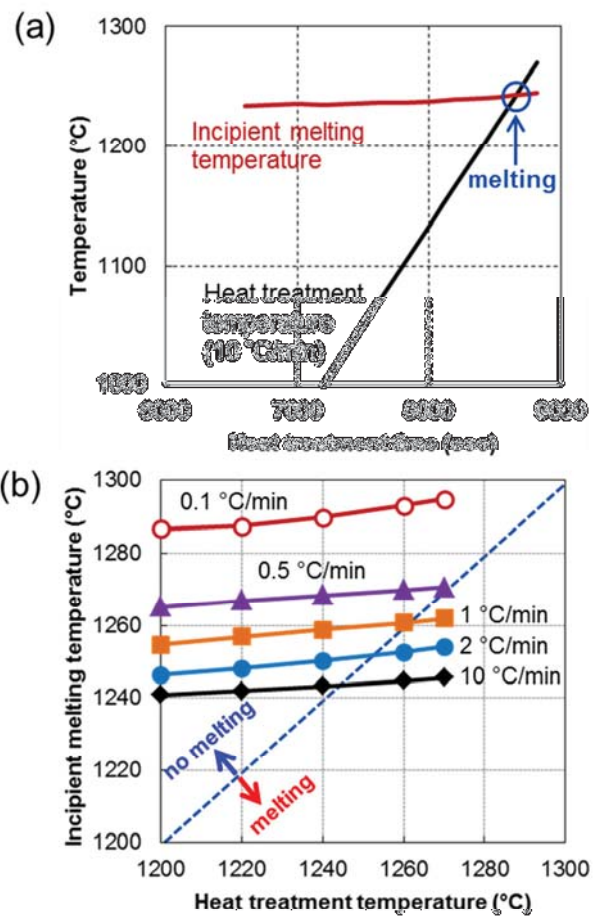

Figure 8. (a) Change in the incipient melting temperature during heating at 10 °C/min and (b) the predicted incipient melting temperatures during heating at various ramp rates to 1270 °C.
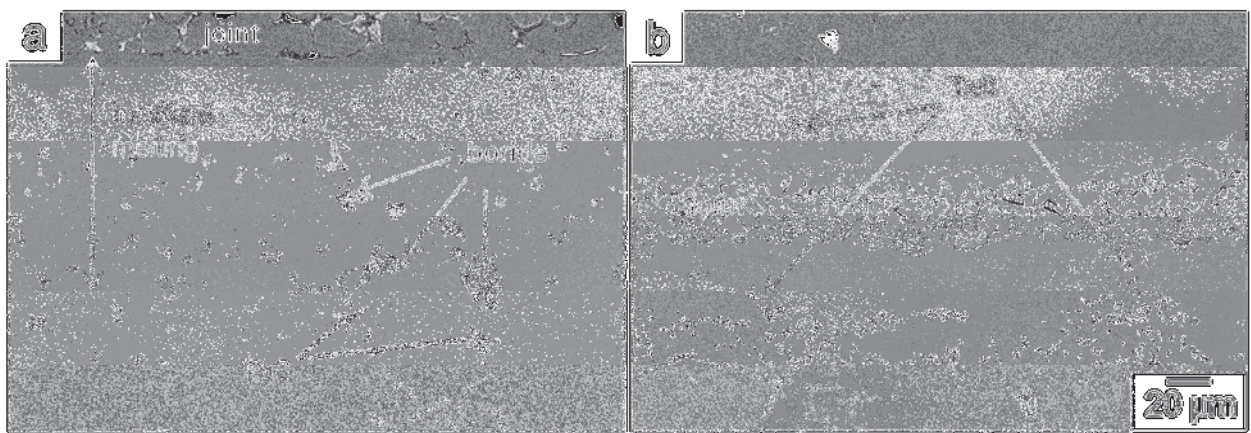

Figure 9. Microstructures of the joined René N5 coupons with the N5+2B interlayer after heating to 1270 °C at (a) 1 °C/min and (b) 0.1 °C/min, followed by water quench.

Figure 8a shows the change in the incipient melting temperature during heating to 1270 °C at 10 °C/min. With heating time, the incipient melting temperature steadily increases as B diffuses out. However, the incipient melting temperature crosses the specimen temperature around 1245 °C, which suggests the onset of incipient melting in the specimen. This prediction is close to the observation shown in Figure 6. Figure 8b shows changes in incipient melting temperatures during heating at various rates. At ramp rates between 1 and 10 °C/min, the increase in the incipient melting temperature was small, and incipient melting was predicted to occur during heating to 1270 °C. At ramp rates below 0.5 °C/min, the incipient melting temperature becomes high enough to avoid incipient melting.

Figure 9 shows a comparison of microstructures heated to 1270 °C at 1 °C/min and 0.1 °C/min, followed by water quench. At 1 °C/min, extensive formation of the eutectic borides was observed near the joint, involving the dissolution of the interdendritic TaC in the substrate (Fig. 9a). On the other hand, at 0.1 °C/min, the interdendritic TaC particles remained intact near the joint, and no formation of the eutectic borides was observed (Fig. 9b). Therefore, by using a slow ramp rate in the second step heat treatment, B can be diffused away to a level that does not cause incipient melting.

Mechanical Properties of the Joined Single-Crystal Superalloy

Mechanical properties of the joints produced by the new joining heat treatment process were evaluated using the René N5 single-crystal superalloy. Tensile tests were conducted at room temperature, 760, 982 and 1093 °C.

Figure 10 summarizes the tensile test results. Two joined specimens were tested at each condition, in comparison with one single-crystal René N5 specimen. Both of the joined specimens showed 0.2 % yield strength, ultimate tensile strength (UTS) and elongation comparable to those of the single-crystal René N5 up to 1093 °C.

Figure 11 shows the pictures of the single-crystal René N5 and the joined René N5 tensile specimens. It is noteworthy that none of the specimens failed at the joints, located in the middle of the gage sections, and that the fracture modes were same as those observed in the single-crystal specimens. These results demonstrate that the new joining process can produce mechanically reliable joints.
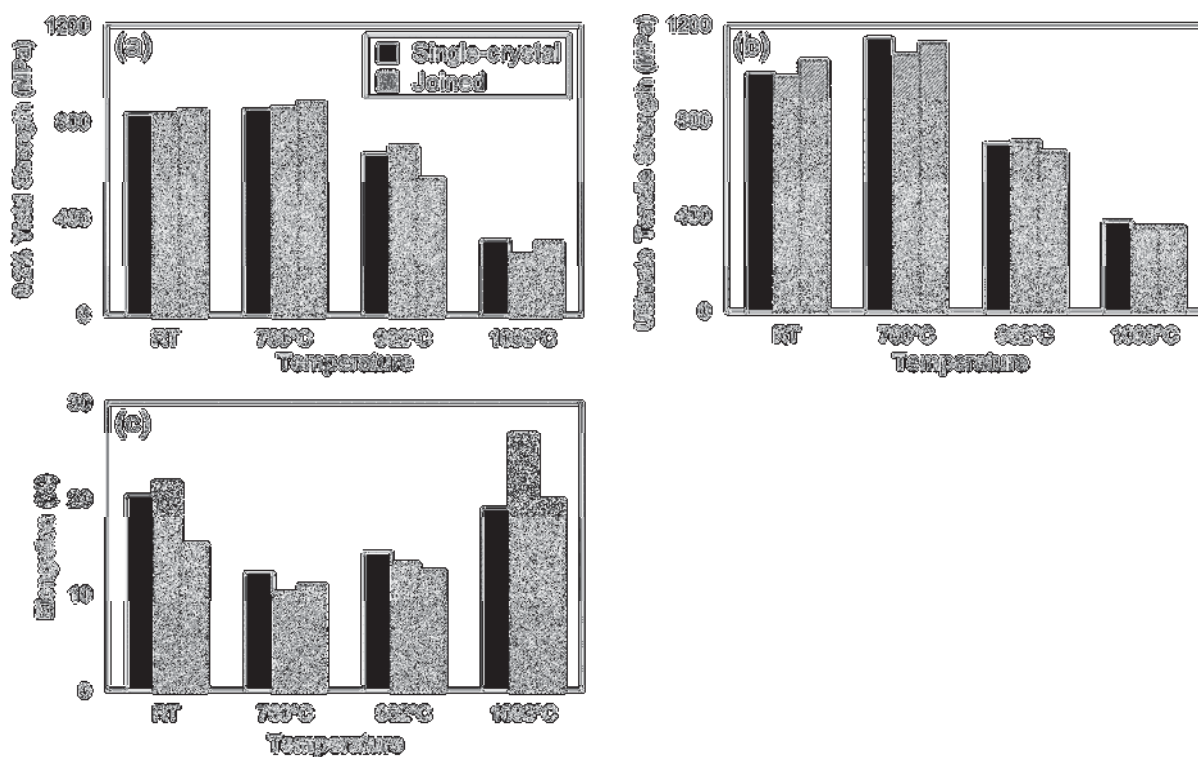

Figure 10. Tensile properties of the joined René N5 in comparison with the single-crystal René N5: (a) 0.2 % yield strength, (b) ultimate tensile strength and (c) elongation.
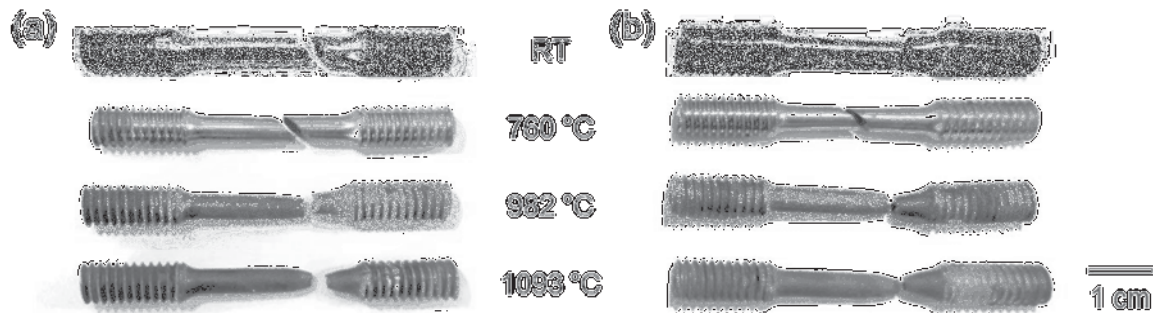
Figure 11. Tensile specimens after testing at RT, 760, 982 and 1093 °C: (a) the single-crystal René N5 and (b) the joined René N5, showing no failure at the joints.

Summary and Conclusions

In this study, microstructure evolution during diffusion brazing was studied using a single-crystal superalloy René N5 and interlayer materials containing B. Based on the observation and the prediction of B diffusion, a new two-step joining heat treatment process route was identified to produce mechanically reliable joints.

1. Due to the fast diffusion of B from the interlayer into the substrate, the interlayer does not fully melt during high temperature joining heat treatment. Solid particles in the partially molten interlayer remain as grains along the joints and become grain defects if they are not eliminated by grain coarsening.

2. To enhance grain coarsening, a two-step joining heat treatment process was developed. During the first step heat treatment at a temperature above the solidus and below the liquidus temperatures of the interlayer, a metallurgical joint is achieved. The grains at the joint remain relatively small due to the relatively low heat treatment temperature. In the second heat treatment at close to or above the γ' solvus temperature of the substrate, the grains at the joint are eliminated by grain coarsening, leaving a joint free of bond line.

3. By using a slow heating rate during the second step heat treatment to diffuse B away from the joint, incipient melting can be avoided. Diffusion calculations can guide optimization of heat treatment conditions.

4. The René N5 specimens joined by the improved joining process demonstrated mechanical reliability at high temperatures. The tensile properties of the joined René N5 were equivalent to those of single-crystal René N5.

Acknowledgement

References

1. D.S. Duvall, W.A. Owczarski, D.F. Paulonis, "TLP Bonding: a New Method for Joining Heat Resistant Alloys," *Welding Journal*, 53 (1974), 203-214.

2. D.M. Jacobson, G. Humpston, *Principles of Brazing* (Materials Park, OH: ASM International, 2005), 207-219.

3. B.B. Seth, P.D. Freyer, M.A. Hebbar, T. Zagar, M.A. Burke, "Cost-Effective Manufacturing of High Performance Power Generation Combustion Turbine Components Using the Fabricated Component Method," *Advances in Turbine Materials, Design and Manufacturing*, ed. A. Strang, W.M. Banks, R.D. Conroy, M.J. Goulette (London, UK: The Institute of Materials, 1997), 129-147.

4. K. Nishimoto, K. Saida, D. Kim, Y. Nakano, "Transient Liquid Phase Bonding of Ni-base Single Crystal Superalloy, CMSX-2," *ISIJ International*, 35 (1995), 1298-1306.

5. K. Nishimoto, K. Saida, D. Kim, S. Asai, Y. Furukawa, Y. Nakao, "Bonding phenomena and joint properties of transient liquid phase bonding of Ni-base single-crystal superalloys," *Welding in the World*, 41 (1998), 121-131.

6. D.-U. Kim, K. Nishimoto,"Creep rupture and fatigue properties of transient liquid phase bonded joints of Ni base single crystal superalloy," *Materials Science and Technology*, 19 (2003), 456-460.

7. B. Laux, S. Piegert, J. Rösler, "Braze Alloy Development for Fast Epitaxial High Temperature Brazing of Single-Crystalline Nickel-Based Superalloys," *Metall. Mater. Trans. A*, 40 (2009), 138-149.

8. B. Laux, J. Rösler, "Development of Ni–Mn-based alloys for the fast epitaxial braze-repair of single-crystalline nickel-based superalloys," *International Journal of Materials Research*, 101 (2010), 614-622.

9. S. Neumeier, M. Dinkel, F. Pyczak, M. Göken, "Nanoindentation and XRD investigations of single-crystalline

Ni-Ge brazed nickel-base superalloys PWA 1483 and René N5," *Materials Science and Engineering A*, 538 (2011), 815-822.

10. H. Ikawa, Y. Nakao, T. Isai, "Theoretical Considerations on the Metallurgical Process in T.L.P. Bonding of Nickel-Base Superalloys," *Transactions of the Japan Welding Society*, 10 (1979), 24-29.

11. O.A. Ojo, N.L Richards, M.C. Chaturvedi, "Isothermal solidification during transient liquid phase bonding of Inconel 738 superalloy," *Science and Technology of Welding and Joining*, 9 (2004), 532-540.

12. F. Jalilian, M. Jahazi., R.A.L. Drew, "Microstructural evolution during transient liquid phase bonding of Inconel 617 using Ni-Si-B filler material," *Materials Science and Engineering A*, 423 (2006), 269-281.

13. M.A. Arafin, M. Medraj, D.P Turner, B. Bocher," Transient liquid phase bonding of Inconel 718 and Inconel 625 with BNi-2: Modeling and experimental Investigations," *Materials Science and Engineering A*, 447 (2007), 125-133.

14. N.P. Wikstrom, A.T. Egbewande, O.A. Ojo, "High temperature diffusion induced liquid phase joining of a heat resistant alloy," *J. Alloys and Compounds*, 460 (2008), 379-385.

15. M.M. Abdelfatah, O.A. Ojo, "On the Extension of Processing Time with Increase in Temperature during Transient-Liquid Phase Bonding," *Metall. Mater. Trans. A*, 40A (2009), 377-385.

16. http://www.thermocalc.com/products-services/databases/thermodynamic/

17. http://www.thermocalc.com/media/6017/dbd_mobni2-2.pdf